Impact of vapor phase Ge incorporation and reaction pathways on the performance and stability of $Cu_2Zn(Ge,Sn)Se_4$ solar cells

Talat Khonsor[a,b,c,*], *David Nowak*[c], *Devendra Pareek*[c], *Maxim Guc*[b], *Robert Fonoll-Rubio*[b], *Victor Izquierdo-Roca*[b], *Pedro Vidal-Fuentes*[b], *Levent Gütay*[c]

a: Electronic Engineering Department, Polytechnic University of Catalonia (UPC), 08034 Barcelona, Spain.

b: Catalonia Institute for Energy Research (IREC), Jardins de les Dones de Negre 1, 2ª pl., 08930 Sant Adrià del Besòs Barcelona, Spain

c: Institute of Physics, Carl von Ossietzky University of Oldenburg, Carl-von-Ossietzky Straße 9-11, 26129 Oldenburg, Germany

Corresponding author email: talat.khonsor@upc.edu

Supplementary Information

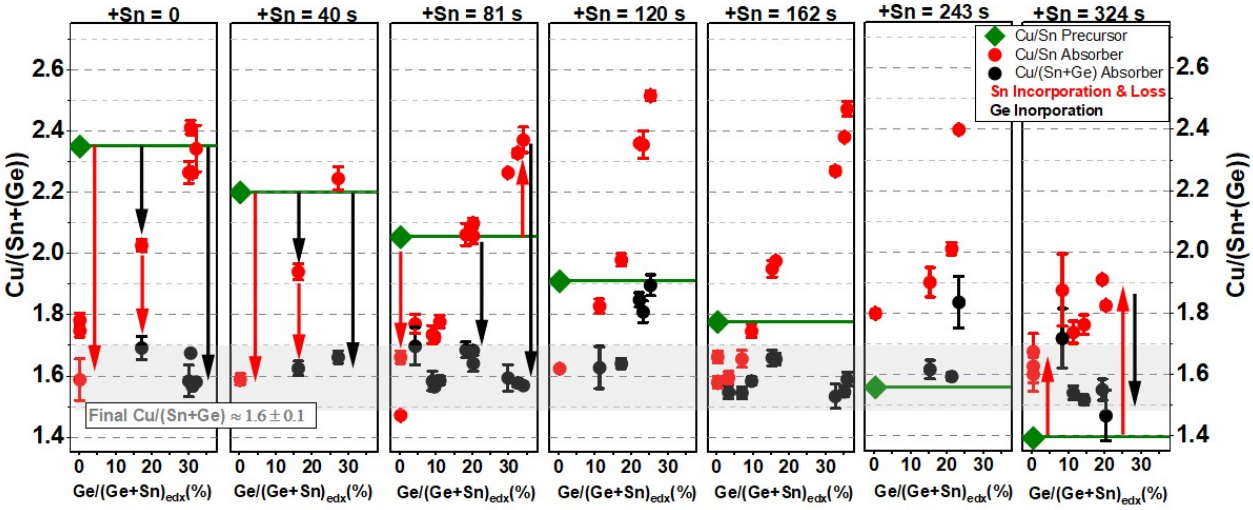

Figure S1. Cu/Sn ratios of both precursors and absorbers, as well as the Cu/(Sn+Ge) ratios of the absorbers, illustrating the composition shift across different Ge content levels and precursor compositions, which were determined by the duration of additional Sn sputtering.

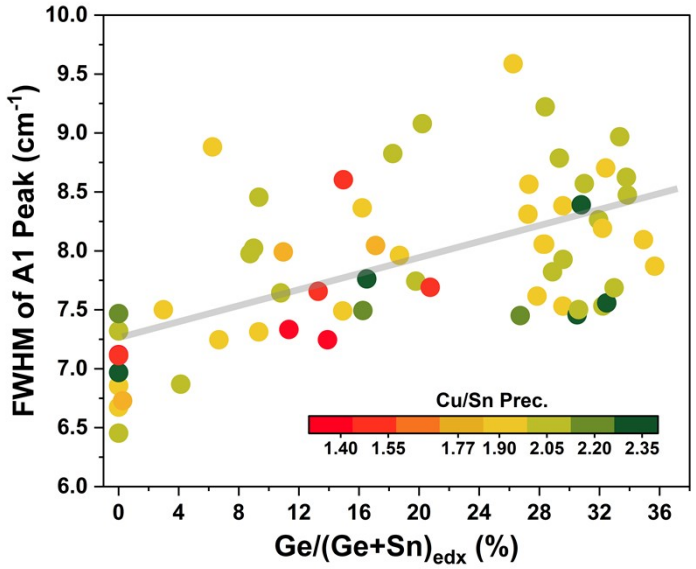

Figure S2. The full width at half maximum (FWHM) of the A1 Raman peak as a function of Ge content for absorbers fabricated from different precursor compositions. A slight broadening of the peak is observed with increasing Ge content.

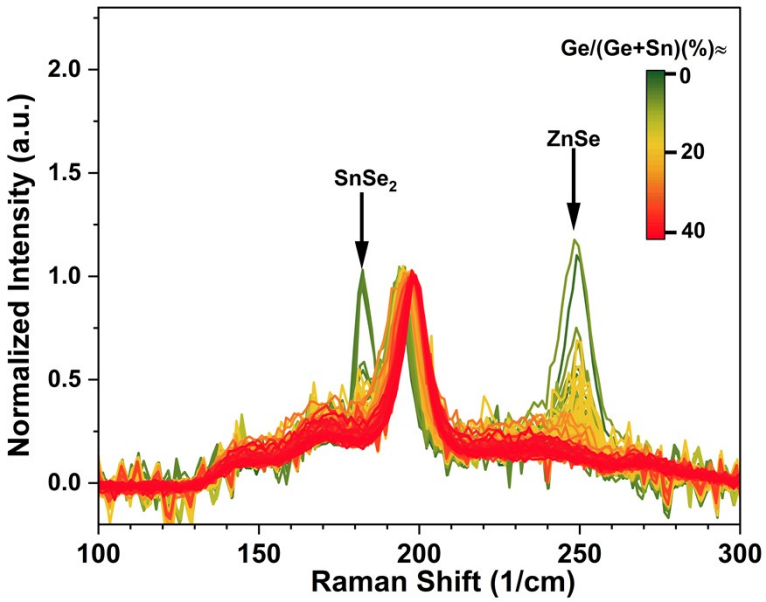

Figure S3. Raman spectra measured under blue laser excitation (457 nm), showing the presence of the ZnSe secondary phase on the surface of some absorbers.

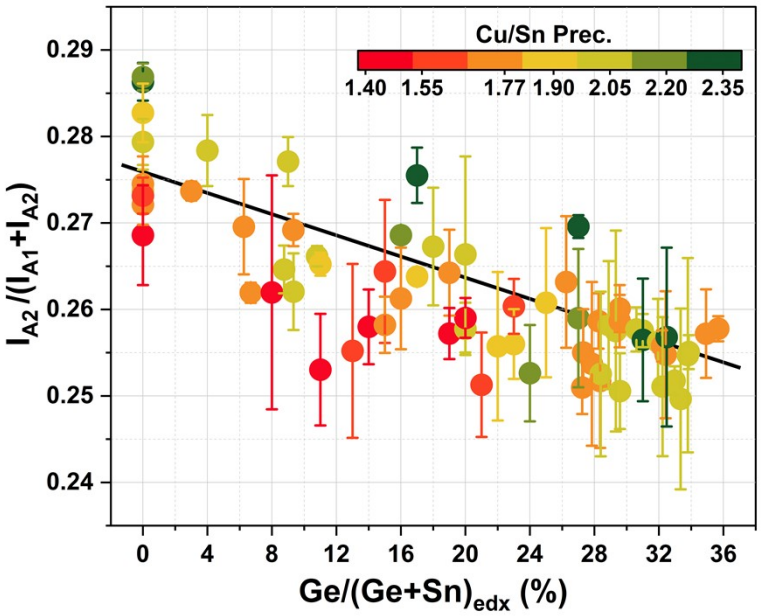

Figure S4. Relative integrated intensities of the A2 Raman peak as a function of Ge content for absorbers fabricated from different precursor compositions.

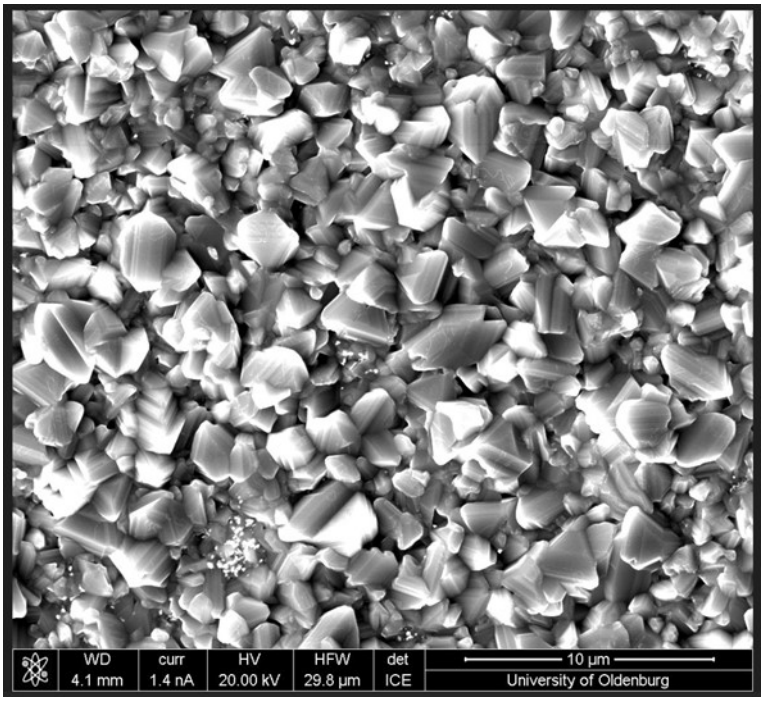

Figure S5. An SEM image of the surface of an absorber, showing the area used for estimating grain size.

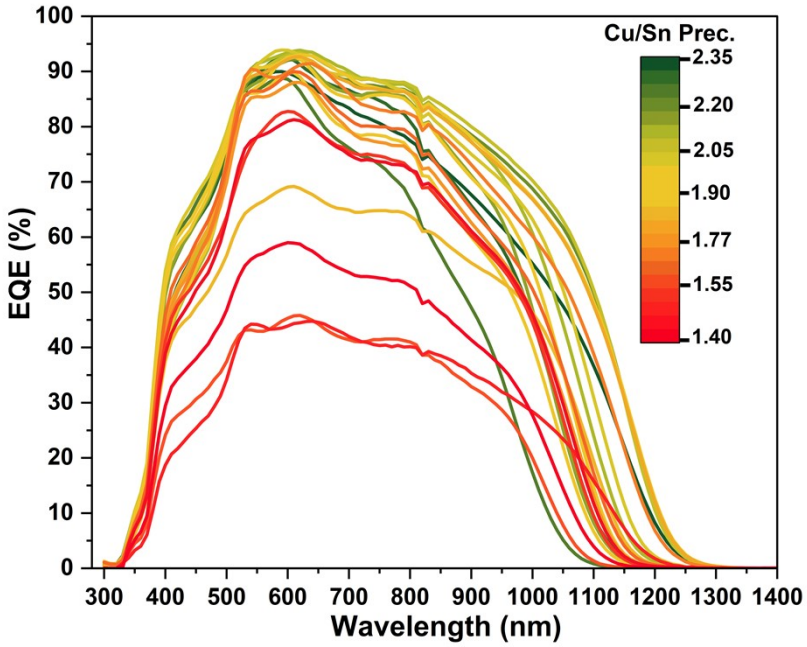

Figure S6. EQE spectra of solar cells synthesized from precursors with varying configurations, particularly different Cu/Sn ratios.

Band gap estimation

In this study, the band gap (E_g) was determined by plotting EQE^2 as a function of energy (E) and performing a linear fit to the linear region of the resulting curve, as illustrated in Fig. S7. The band gap was then defined as the x-axis intercept of this fitted line.

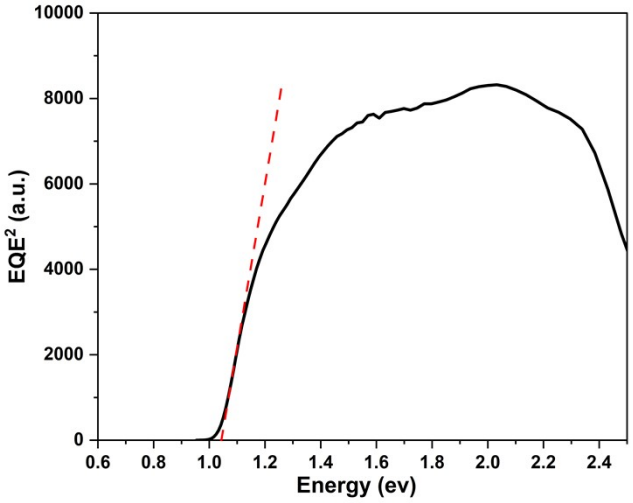

Figure S7. Illustration of the graph used to determine the material's band gap from the EQE measurement data.

Urbach energy

In this study, the Urbach energy (E_u) was quantitatively estimated based on the empirical relationship between the absorption coefficient and Urbach energy, as reported in Ref. [1]. This was done by plotting ln(EQE) as a function of photon energy (e.g., Fig. S8). In the resulting graph, the linear region just below the band gap energy was identified and fitted. The slope of this linear fit was then used to determine the Urbach energy, as it is inversely proportional to E_u.

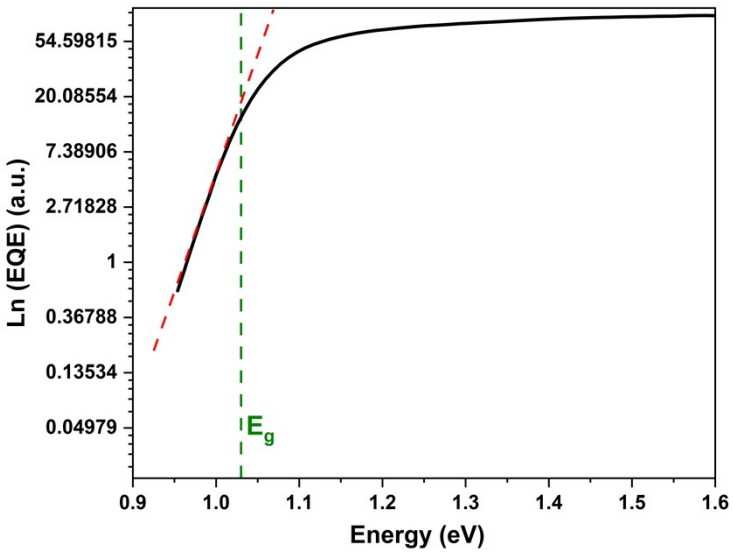

Figure S8. Illustration of the graph and method used to estimate the Urbach energy from EQE measurement data.

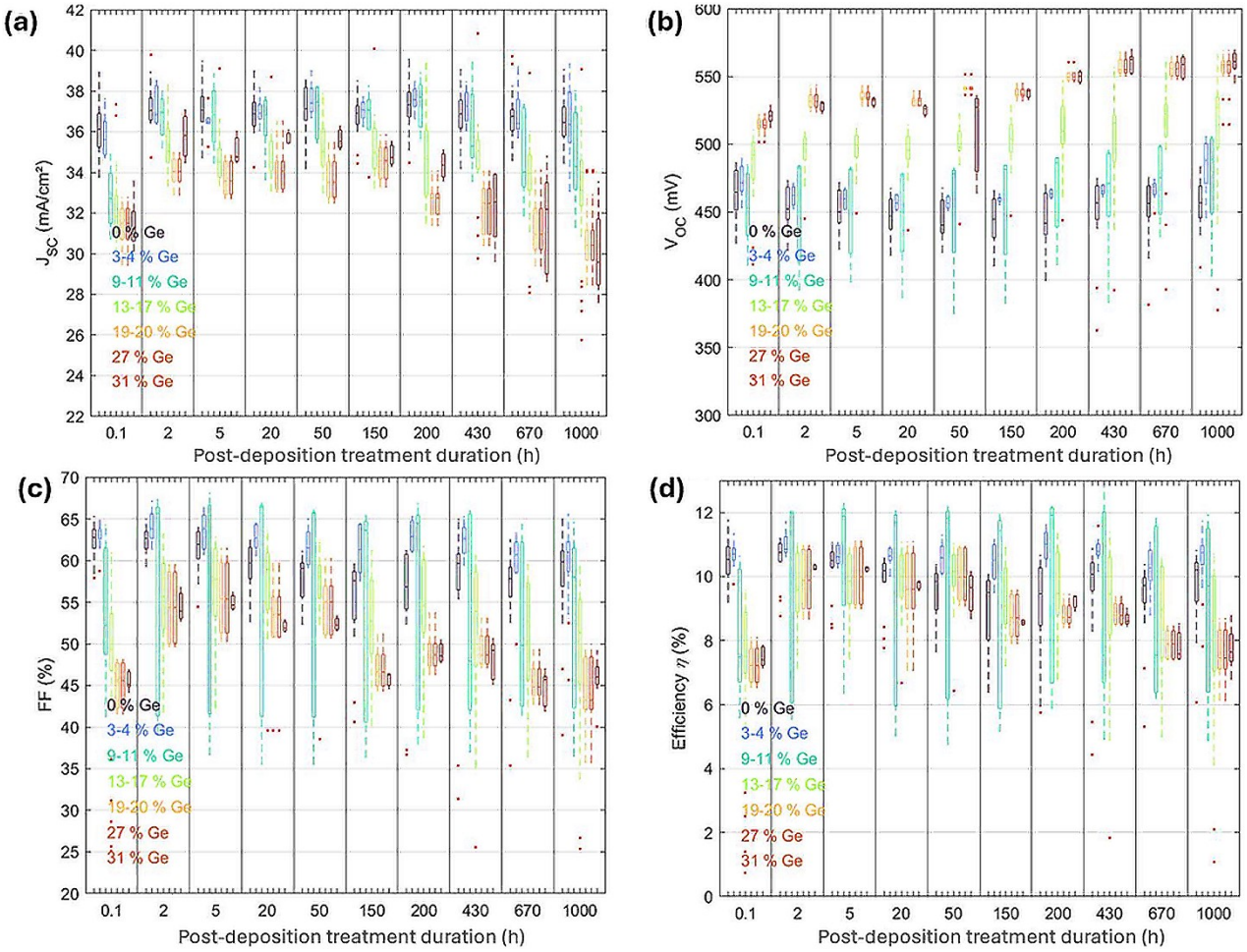

Figure S9. Changes in the standard solar cell parameters (J_{sc}, V_{oc}, FF, and efficiency) during the controlled post-deposition heat treatment experiment.

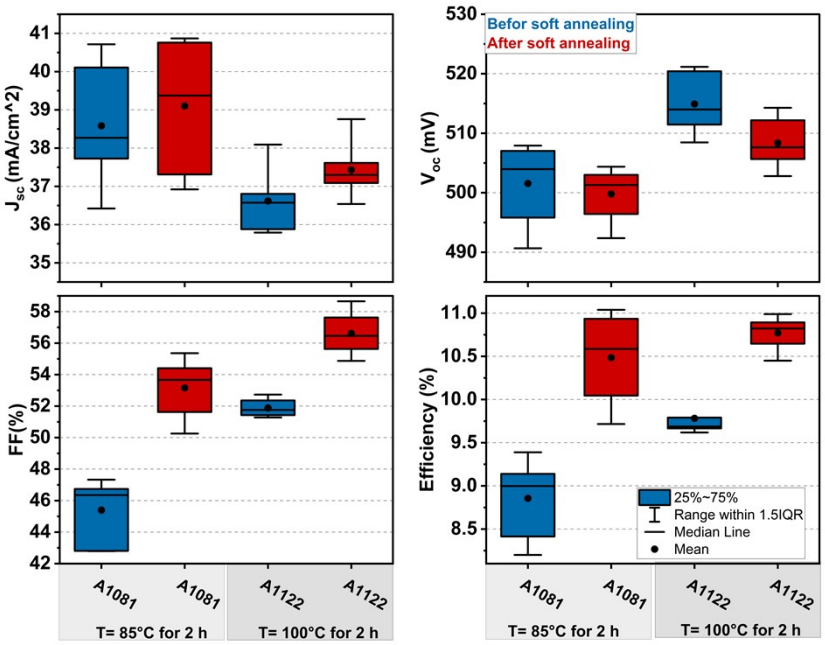

Figure S10. Comparison of the standard solar cell parameters (J_{sc}, V_{oc}, FF, and efficiency) for Ge-containing devices before and after soft annealing for 2 h at different annealing temperatures (85 °C and 100 °C).

References

1 F. Urbach, *Phys. Rev.*, **1953**, *92*, 1324.